

NASA Contractor Report 178375

ICASE REPORT NO. 87-64

ICASE

**DISCONTINUOUS SOLUTIONS TO HYPERBOLIC
SYSTEMS UNDER OPERATOR SPLITTING**

P. L. Roe

**(NASA-CR-178375) DISCONTINUOUS SOLUTIONS TO
HYPERBOLIC SYSTEMS UNDER OPERATOR SPLITTING
Final Report (NASA) 35 p Avail: NTIS HC
A03/MF A01**

N87-29785

CSCL 200

G3/34 0100130

Unclas

**Contract No. NAS1-18107
September 1987**

**INSTITUTE FOR COMPUTER APPLICATIONS IN SCIENCE AND ENGINEERING
NASA Langley Research Center, Hampton, Virginia 23665**

Operated by the Universities Space Research Association



**National Aeronautics and
Space Administration**

**Langley Research Center
Hampton, Virginia 23665**

**DISCONTINUOUS SOLUTIONS TO HYPERBOLIC SYSTEMS
UNDER OPERATOR SPLITTING**

P. L. Roe
Cranfield Institute of Technology, UK

ABSTRACT

Two-dimensional systems of linear hyperbolic equations are studied with regard to their behavior under a solution strategy that in alternate time-steps solves exactly the component one-dimensional operators. The initial data is a step function across an oblique discontinuity. The manner in which this discontinuity breaks up under repeated applications of the split operator is analyzed, and it is shown that the split solution will fail to match the true solution in any case where the two operators do not share all their eigenvectors. The special case of the fluid flow equations is analyzed in more detail, and it is shown that arbitrary initial data gives rise to "pseudo acoustic waves" and a non-physical stationary wave. The implications of these findings for the design of high-resolution computing schemes are discussed.

This research was supported under the National Aeronautics and Space Administration under NASA Contract No. NAS1-18107 while the author was in residence at the Institute for Computer Applications in Science and Engineering (ICASE), NASA Langley Research Center, Hampton, VA 23665.

1. INTRODUCTION

This paper is concerned with two-dimensional systems of time-dependent partial differential equations. We write these in their matrix form

$$\tilde{u}_t + A\tilde{u}_x + B\tilde{u}_y = 0, \quad (1.1)$$

and restrict our attention to the hyperbolic case, characterized by the fact that the $n \times n$ matrix $(A \cos \phi + B \sin \phi)$ possesses a full set of independent eigenvectors for all angles ϕ . Physically this corresponds to the fact that for any direction ϕ it is possible to construct n different families of plane wave solutions travelling in that direction.

A common technique for solving (1.1) numerically is that of operator splitting. The operation of advancing (1.1) through a time interval Δt is replaced, in the simplest case, by the following two operations. First the data is advanced by $\frac{1}{2} \Delta t$ by means of the one-dimensional operator

$$\tilde{u}_t + 2A\tilde{u}_x = 0, \quad (1.2)$$

and then the new solution is advanced through $\frac{1}{2} \Delta t$ by means of

$$\tilde{u}_t + 2B\tilde{u}_y = 0. \quad (1.3)$$

Repetition of this pair of operators N times is assumed to be equivalent to advancing (1.1) by $N\Delta t$. The attraction of the strategy is that it allows use to be made of very accurate and sophisticated one-dimensional numerical schemes. The drawback is that the splitting itself introduces errors,

proportional in the above case to Δt (although different sequences of split operators reduce this to $(\Delta t)^2$) even into a smooth flow [1].

Crandall and Majda [2] have pointed out additional errors that arise when the problem is nonlinear, albeit scalar. Singularities of the solution may be shocks, expansions, or contacts, corresponding to converging, diverging, or parallel characteristics. The errors occur when a singularity of one type is misread as being of another type by either of the one-dimensional operators.

The error discussed in this paper is also a misreading, arising even at the linear level if there is more than one unknown. A and B are then constant matrices, and the problem is found whenever the eigenvectors of A are different from the eigenvectors of B. In that case, we will show the consequences of operator splitting when the initial discontinuity consists of a single oblique discontinuity and each of the one-dimensional split problems is solved exactly. The results do not therefore relate to any particular numerical scheme, but can be used to explain certain anomalies that are observed in practice, and to suggest the kind of scheme that can be employed in given problems. A qualitative version of the analysis was given by Colella [3], but the present treatment reveals additional detail.

We will study two specific cases. One of these is the 2×2 system

$$\begin{vmatrix} u \\ v \end{vmatrix}_t + \begin{vmatrix} 1 & 0 \\ 0 & -1 \end{vmatrix} \begin{vmatrix} u \\ v \end{vmatrix}_x + \begin{vmatrix} 0 & 1 \\ 1 & 0 \end{vmatrix} \begin{vmatrix} u \\ v \end{vmatrix}_y = 0, \quad (1.4)$$

and the other is the 4×4 system

$$\begin{vmatrix} p \\ u \\ v \\ s \end{vmatrix}_t + \begin{vmatrix} u & \rho a^2 & 0 & 0 \\ 1/\rho & u & 0 & 0 \\ 0 & 0 & u & 0 \\ 0 & 0 & 0 & u \end{vmatrix} \begin{vmatrix} p \\ u \\ v \\ s \end{vmatrix}_x + \begin{vmatrix} v & 0 & \rho a^2 & 0 \\ 0 & v & 0 & 0 \\ 1/\rho & 0 & v & 0 \\ 0 & 0 & 0 & v \end{vmatrix} \begin{vmatrix} p \\ u \\ v \\ s \end{vmatrix}_y = 0. \quad (1.5)$$

The first of these is an abstract system that serves to introduce the methodology; the second is a linear version of the compressible flow (Euler) equations, using pressure, velocity and entropy as unknowns.

In Section 2 and 3 we will briefly recall the time evolution of an oblique initial discontinuity in the data (Riemann problem). In Sections 4 and 5 we calculate how such a discontinuity evolves under the split operators when the governing equations are respectively (1.4) and (1.5). Section 6 contains numerical examples, and Section 7 discusses the implications.

2. THE EXACT SOLUTION

Consider initial data in which states u_L, u_R occupy semi-infinite regions separated by a straight line inclined at an angle ϕ (Fig. 1(a)). Introducing coordinates x', y' as shown (1.1) becomes

$$u_t + (A \cos \phi + B \sin \phi) u_{x'} + (A \sin \phi - B \cos \phi) u_{y'} = 0. \quad (2.1)$$

Solutions not depending on y' having the form

$$u = f(x' - \lambda t) r$$

can be found if λ is an eigenvalue of $(A \cos \phi + B \sin \phi)$, and if r is the corresponding eigenvector. By a limiting process we can justify taking f to be the Heaviside function. To solve the proposed problem, project the given jump onto the eigenvectors

$$u_R - u_L = \sum_{i=1}^{i=n} \alpha_i(\phi) r_i(\phi). \quad (2.2)$$

In terms of Heaviside functions, the data is

$$u = u_L + \sum_{i=1}^{i=n} \alpha_i(\phi) H(x^-) r_i(\phi), \quad (2.3)$$

and the solution at time t is (see Fig. 1b)

$$u = u_L + \sum_{i=1}^{i=n} \alpha_i(\phi) H(x^- - \lambda_i t) r_i(\phi). \quad (2.4)$$

Our object is to discover how well the split operators reproduce this exact solution.

3. THE OPERATOR-SPLIT SOLUTION

During those periods when the equation being solved is (1.2), any jumps in the solution are eigenvectors of A . If this equation is used to evolve the initial data, the result is

$$u = u_L + \sum_{i=0}^{i=n} \alpha_i(0) H(x^- \cos \phi - 2\lambda_i(0)t) r_i(0). \quad (3.1)$$

Similarly, if we use (1.3), we obtain

$$u = u_L + \sum_{i=0}^{i=n} \alpha_i\left(\frac{1}{2}\pi\right) H(x^- \sin \phi - 2\lambda_i\left(\frac{1}{2}\pi\right)t) r_i\left(\frac{1}{2}\pi\right). \quad (3.2)$$

Now suppose that the initial discontinuity evolves for $\frac{1}{2} \Delta t$ according to (1.2). It will generate n distinct wavefronts (Fig. 2a shows the case $n = 2$). Each of these generates new data to be evolved for a further $\frac{1}{2} \Delta t$ according to (1.3). At the end of the second interval we will have n^2 waves in the system. After time $k\Delta t$ we would have $n^{(2k)}$ waves.

4. THE ABSTRACT SYSTEM

Here the problem

$$\underline{u}_t + A\underline{u}_x + B\underline{u}_y = 0 \quad (4.1)$$

is defined by

$$\underline{u} = \begin{bmatrix} u \\ v \end{bmatrix}, \quad A = \begin{bmatrix} 1 & 0 \\ 0 & -1 \end{bmatrix}, \quad B = \begin{bmatrix} 0 & 1 \\ 1 & 0 \end{bmatrix}. \quad (4.2)$$

The eigenvalues of $A \cos \phi + B \sin \phi$ satisfy

$$\det \begin{vmatrix} \cos \phi - \lambda & \sin \phi \\ \sin \phi & -(\cos \phi + \lambda) \end{vmatrix} = 0, \quad (4.2)$$

i.e.,

$$\lambda^2 = 1. \quad (4.3)$$

Denoting by $\underline{r}^\pm(\phi)$ the eigenvectors for $\lambda = \pm 1$, we obtain

$$\underline{r}^-(\phi) = \begin{bmatrix} -\sin \frac{1}{2} \phi \\ \cos \frac{1}{2} \phi \end{bmatrix}, \quad \underline{r}^+(\phi) = \begin{bmatrix} \cos \frac{1}{2} \phi \\ \sin \frac{1}{2} \phi \end{bmatrix}. \quad (4.4)$$

In particular,

$$\underline{r}^-(0) = \begin{bmatrix} 0 \\ 1 \end{bmatrix}, \quad \underline{r}^+(0) = \begin{bmatrix} 1 \\ 0 \end{bmatrix}, \quad (4.5)$$

and

$$r^-(\frac{1}{2}\pi) = \begin{vmatrix} -1/\sqrt{2} \\ 1/\sqrt{2} \end{vmatrix} \quad r^+(\frac{1}{2}\pi) = \begin{vmatrix} 1/\sqrt{2} \\ 1/\sqrt{2} \end{vmatrix}. \quad (4.6)$$

If these eigenvectors are denoted by $\tilde{r}_x^-, \tilde{r}_x^+, \tilde{r}_y^-, \tilde{r}_y^+$, we have the identities

$$\begin{aligned} \tilde{r}_x^+ &= \frac{1}{\sqrt{2}} (\tilde{r}_y^+ - \tilde{r}_y^-), \\ \tilde{r}_x^- &= \frac{1}{\sqrt{2}} (\tilde{r}_y^- + \tilde{r}_y^+), \\ \tilde{r}_y^+ &= \frac{1}{\sqrt{2}} (\tilde{r}_x^- + \tilde{r}_x^+), \\ \tilde{r}_y^- &= \frac{1}{\sqrt{2}} (\tilde{r}_x^+ - \tilde{r}_x^-). \end{aligned} \quad (4.7)$$

For example, we see that at the end of an x-step, each \tilde{r}_x^+ wave will give rise to \tilde{r}_y^+ and \tilde{r}_y^- waves of amplitudes respectively $1/\sqrt{2}$ and $-1/\sqrt{2}$ times that of the source wave. To develop the notation further we introduce translation operators C and S, corresponding to translation of a wavefront in the x'-direction by $\Delta t \cos \phi$ and $\Delta t \sin \phi$. We use notation (\Rightarrow) to mean "gives rise to" and derive from (4.7)

$$\begin{aligned} \tilde{r}_x^+ &\Rightarrow \frac{1}{\sqrt{2}} (S \tilde{r}_y^+ - S^{-1} \tilde{r}_y^-), \\ \tilde{r}_x^- &\Rightarrow \frac{1}{\sqrt{2}} (S^{-1} \tilde{r}_y^- + S \tilde{r}_y^+), \\ \tilde{r}_y^+ &\Rightarrow \frac{1}{\sqrt{2}} (C^{-1} \tilde{r}_x^- + C \tilde{r}_x^+), \\ \tilde{r}_y^- &\Rightarrow \frac{1}{\sqrt{2}} (C^{-1} \tilde{r}_x^+ - C \tilde{r}_x^-). \end{aligned} \quad (4.8)$$

This produces a calculus for tracing the history of a wave through any number of split operations. Thus, an r_x^+ wave, operated on first in the x- and then the y-direction, evolves according to

$$\begin{aligned}
 r_x^+ &\Rightarrow \frac{1}{\sqrt{2}} (S r_y^+ - S^{-1} \tilde{r}_y^-) \\
 &\Rightarrow \frac{1}{2} [S(C^{-1} \tilde{r}_x^- + C r_x^+) - S^{-1}(C^{-1} r_x^- - C r_x^+)] \\
 &= \frac{1}{2} (SC + S^{-1}C) \tilde{r}_x^+ + \frac{1}{2} (SC^{-1} - S^{-1}C^{-1}) \tilde{r}_x^-.
 \end{aligned} \tag{4.9}$$

Similarly, under the same operations

$$r_x^- \Rightarrow \frac{1}{2} (SC - S^{-1}C) \tilde{r}_x^+ + \frac{1}{2} (SC^{-1} + S^{-1}C^{-1}) \tilde{r}_x^-. \tag{4.10}$$

A powerful notation to describe the configuration of waves present after a certain number of steps is to introduce a vector $\tilde{a} = (a_1, a_2)^T$ each of whose components is a sum of terms $k_{\alpha\beta} S^\alpha C^\beta$. Such a term describes a wave of amplitude $k_{\alpha\beta}$ at a location $x' = \alpha \sin \phi + \beta \cos \phi$. We use a_1 to describe the \tilde{r}_x^+ waves and a_2 to describe the \tilde{r}_x^- waves. Evolution through a pair of split operations from $k\Delta t$ to $(k+1)\Delta t$ can then be described as

$$\tilde{a}_{k+1} = M \tilde{a}_k. \tag{4.11}$$

where the matrix M can be obtained from (4.9), (4.10) as

$$M = \begin{vmatrix} \frac{1}{2} (SC + S^{-1}C) & \frac{1}{2} (SC - S^{-1}C) \\ \frac{1}{2} (SC^{-1} - S^{-1}C^{-1}) & \frac{1}{2} (SC^{-1} + S^{-1}C^{-1}) \end{vmatrix}. \tag{4.12}$$

The equation

$$\tilde{a}_k = M^k \tilde{a}_0 \quad (4.13)$$

is then a formal solution to the initial-value problem, if $\tilde{a}_0 = (\alpha^+, \alpha^-)^T$ where α^+, α^- are the projections of the initial jump onto the eigenvectors \tilde{x}_λ^\pm . However, computing high powers of M would be cumbersome, and it is more convenient to use the recurrence relationship

$$\tilde{a}_k = \text{tr}(M)\tilde{a}_{k-1} - \det(M)\tilde{a}_{k-2}. \quad (4.14)$$

This follows from applying to \tilde{a}_{k-2} the identity

$$M^2 - \text{tr}(M)M + \det(M)I = 0$$

which is the form taken for $n = 2$ by the Cayley-Hamilton theorem. Applying (4.14) to (4.12) gives

$$\tilde{a}_k = \frac{1}{2} (S + S^{-1})(C + C^{-1})\tilde{a}_{k-1} - \tilde{a}_{k-2}. \quad (4.15)$$

The iteration need not start with an isolated discontinuity, but may take \tilde{a}_0 arbitrary, $\tilde{a}_1 = M\tilde{a}_0$.

A particularly simple case that yields more general insights is to take $\phi = \frac{1}{4}\pi$, so that $S = C = T$ (say) so that

$$\tilde{a}_k = \frac{1}{2} (T^2 + 2 + T^{-2})\tilde{a}_{k-1} - \tilde{a}_{k-2}. \quad (4.16)$$

Let \tilde{c}_n^k be the coefficient of T^k in \tilde{a}_k . Then (4.16) translates to

$$\tilde{c}_n^{k+1} = \tilde{c}_n^k + \frac{1}{2} (\tilde{c}_{n-2}^k + \tilde{c}_{n+2}^k) - \tilde{c}_n^{k+1}, \quad (4.17)$$

or, rearranging

$$\tilde{c}_n^{k+1} - 2\tilde{c}_n^k + \tilde{c}_n^{k-1} = \frac{1}{2} (\tilde{c}_{n-2}^k - 2\tilde{c}_n^k + \tilde{c}_{n+2}^k). \quad (4.18)$$

This shows that \tilde{c}_n^k behaves like a leapfrog approximation to the wave equation

$$\tilde{c}_{tt} = 2\tilde{c}_{xx} = \tilde{c}_{x'x'}. \quad (4.19)$$

The approximation has an effective Courant number of $1/\sqrt{2}$. In (4.19) we see waves propagating to left and right with unit velocity as in the exact solution, but in (4.18) we will expect the phase error and oscillations that typify leapfrog schemes.

The precise nature of the phase errors can be found by subjecting (4.18) to the usual Fourier analysis via the ansatz

$$\tilde{c}_n^k = g^k \exp(i\theta x'/\Delta t) \quad (4.20)$$

where g is a complex amplification factor, and θ is the Fourier frequency. Substituting (4.20) into (4.18) yields

$$g^2 - 2g \cos(\theta \sin \phi) \cos(\theta \cos \phi) + 1 = 0 \quad (4.21)$$

or

$$g = \cos(\theta \sin \phi) \cos(\theta \sin \phi) \pm i[1 - \cos^2(\theta \sin \phi) \cos^2(\theta \cos \phi)]^{1/2}. \quad (4.22)$$

Since $|g| = 1$ there is no dissipation. The phase shift per iteration is given by

$$\tan^{-1} \frac{[1 - \cos^2(\theta \sin \phi) \cos^2(\theta \cos \phi)]^{1/2}}{\cos(\theta \sin \phi) \cos(\theta \cos \phi)} \quad (4.22)$$

which equals θ whenever $\phi = N\pi/2$. For other values of ϕ , (4.22) can be expanded in θ to give a phase velocity of

$$\frac{\sin^2 2\phi}{24} \theta^2 + O(\theta^4). \quad (4.23)$$

Since the operator-splitting solution has emerged as a nondissipative second-order approximation to the exact solution (for plane waves) standard results for such schemes apply. In particular, an initial discontinuity will be dispersed over an area proportional to $t^{1/3}$, and the accompanying overshoots will reach a maximum amplitude of 27% of the initial amplitude [4].

5. THE LINEARIZED EULER EQUATIONS

In this section the problem

$$\tilde{u}_t + A\tilde{u}_x + B\tilde{u}_y = 0 \quad (5.1)$$

is defined by

$$u = \begin{bmatrix} p \\ u \\ v \\ s \end{bmatrix}, \quad A = \begin{bmatrix} u & \rho a^2 & 0 & 0 \\ 1/\rho & u & 0 & 0 \\ 0 & 0 & u & 0 \\ 0 & 0 & 0 & u \end{bmatrix}, \quad B = \begin{bmatrix} v & 0 & \rho a^2 & 0 \\ 0 & v & 0 & 0 \\ 1/\rho & 0 & v & 0 \\ 0 & 0 & 0 & v \end{bmatrix}. \quad (5.2)$$

The eigenvalues of $(A \cos \phi + B \sin \phi)$ are the roots of

$$\det \begin{vmatrix} U - \lambda & \rho a \cos \phi & \rho a \sin \phi & 0 \\ \cos \phi / \rho & U - \lambda & 0 & 0 \\ \sin \phi / \rho & 0 & U - \lambda & 0 \\ 0 & 0 & 0 & U - \lambda \end{vmatrix} = 0 \quad (5.3)$$

where $U = u \cos \phi + v \sin \phi$, i.e.,

$$(U - \lambda)^2 [(U - \lambda)^2 - a^2] = 0. \quad (5.4)$$

Corresponding to the two eigenvalues $\lambda = U$ are eigenvectors

$$\tilde{r}_s = \begin{vmatrix} 0 \\ 0 \\ 0 \\ 1 \end{vmatrix}, \quad (5.5)$$

describing an entropy wave, and

$$\tilde{r}_v = \begin{vmatrix} 0 \\ -\sin \theta \\ \cos \theta \\ 0 \end{vmatrix}, \quad (5.6)$$

called here a vorticity wave, across which the tangential component of velocity changes.

Corresponding to the eigenvalue $\lambda = U + a$ is an eigenvector

$$\tilde{r}_a = \begin{vmatrix} \rho a \\ \cos \theta \\ \sin \theta \\ 0 \end{vmatrix} \quad (5.7)$$

which describes an acoustic wave. If θ ranges over $[-\pi, \pi]$ in (5.7), the eigenvalue $\lambda = U - a$ is accounted for as well.

With no real loss of generality we can assume that the linearization is about a state of rest (both the exact and operator-split solutions are invariant under steady translations). In that case the entropy and vorticity waves are stationary, and the acoustic waves can move with the sound speed a in any direction (ϕ) .

To find the effect of the split operators we need to take $\phi = 0, \frac{1}{2} \pi$, yielding

$$\tilde{r}_{sx} = \begin{bmatrix} 0 \\ 0 \\ 0 \\ 1 \end{bmatrix}, \tilde{r}_{vx} = \begin{bmatrix} 0 \\ 0 \\ 1 \\ 0 \end{bmatrix}, \tilde{r}_{ax}^+ = \begin{bmatrix} \rho a \\ 1 \\ 0 \\ 0 \end{bmatrix}, \tilde{r}_{ax}^- = \begin{bmatrix} \rho a \\ -1 \\ 0 \\ 0 \end{bmatrix}, \quad (5.8)$$

$$\tilde{r}_{sy} = \begin{bmatrix} 0 \\ 0 \\ 0 \\ 1 \end{bmatrix}, \tilde{r}_{vy} = \begin{bmatrix} 0 \\ -1 \\ 0 \\ 0 \end{bmatrix}, \tilde{r}_{ay}^+ = \begin{bmatrix} \rho a \\ 0 \\ 1 \\ 0 \end{bmatrix}, \tilde{r}_{ay}^- = \begin{bmatrix} \rho a \\ 0 \\ -1 \\ 0 \end{bmatrix}. \quad (5.9)$$

The following identities determine how each time split wave will fission into waves travelling in the other direction

$$\tilde{r}_{sx} = \tilde{r}_{sy}$$

$$\tilde{r}_{vx} = \frac{1}{2} [\tilde{r}_{ay}^+ - \tilde{r}_{ay}^-] \quad (5.10)$$

$$\tilde{r}_{ax}^+ = \frac{1}{2} [\tilde{r}_{ay}^+ + \tilde{r}_{ay}^-] - \tilde{r}_{vy}$$

$$\tilde{r}_{ax}^- = \frac{1}{2} [\tilde{r}_{ay}^+ + \tilde{r}_{ay}^-] + \tilde{r}_{vy}$$

$$\tilde{r}_{sy} = \tilde{r}_{sx}$$

$$\tilde{r}_{vy} = \frac{1}{2} [\tilde{r}_{ax}^- - \tilde{r}_{ax}^+] \quad (5.11)$$

$$\tilde{r}_{ay}^+ = \frac{1}{2} [\tilde{r}_{ax}^- + \tilde{r}_{ax}^+] + \tilde{r}_{vx}$$

$$\tilde{r}_{ay}^- = \frac{1}{2} [\tilde{r}_{ax}^- + \tilde{r}_{ax}^+] - \tilde{r}_{vx}.$$

From these results we can determine the evolution matrix for this problem. Let \tilde{a} be a four-vector whose components describe the configurations of waves \tilde{r}_x^+ , \tilde{r}_x^- , \tilde{r}_v , and \tilde{r}_s respectively. Then some algebra reveals that

$$\tilde{a}_{k+1} = M \tilde{a}_k, \quad (5.12)$$

where

$$M = \begin{vmatrix} \frac{1}{4} (S + S^{-1} + 2)C & \frac{1}{4} (S + S^{-1} - 2)C & \frac{1}{4} (S - S^{-1})C & 0 \\ \frac{1}{4} (S + S^{-1} - 2)C^{-1} & \frac{1}{4} (S + S^{-1} + 2)C^{-1} & \frac{1}{4} (S - S^{-1})C^{-1} & 0 \\ \frac{1}{2} (S - S^{-1}) & \frac{1}{2} (S - S^{-1}) & \frac{1}{2} (S + S^{-1}) & 0 \\ 0 & 0 & 0 & 1 \end{vmatrix} \quad (5.13)$$

and S, C represent displacements through $a\Delta t \sin\phi$, $a\Delta t \cos\phi$.

The most obvious feature of (5.13) is that the entropy waves (at this linearized level) decouple completely from the rest of the waves, and are in fact represented exactly in the operator-split solution. It is easy to see that these statements are always true of any wave that is an eigenvector of both A and B (and hence of $A \cos\phi + B \sin\phi$).

The matrix (5.13) has another property not observed in the earlier problem (4.12). By treating S and C formally as real variables, we can

attempt to find eigenvalues of M . It is quite clear that there will be one eigenvalue $\Lambda = 1$, with eigenvector $(0, 0, 0, 1)^T$ corresponding to a configuration that is a steady solution of the system. The cubic that gives the other eigenvalues is

$$(\Lambda^3 - 1) - (\Lambda^2 - \Lambda) \left[\frac{1}{2} (S + S^{-1}) + \frac{1}{4} (S + S^{-1} + 2)(C + C^{-1}) \right] = 0. \quad (5.14)$$

The existence of a second unit eigenvalue $\Lambda = 1$ implies another steady-state configuration. The corresponding eigenvector

$$p = \begin{vmatrix} C^{1/2}(S^{1/2} - S^{-1/2}) \\ -C^{-1/2}(S^{1/2} - S^{-1/2}) \\ (C^{-1/2} - C^{1/2})(S^{1/2} + S^{-1/2}) \\ 0 \end{vmatrix} \quad (5.15)$$

itself exactly. (The other roots Λ_2, Λ_3 of (5.14) are pseudo-operators, having no simple interpretations, although we may remark that $\Lambda_2 \Lambda_3 = 1$. In this sense, they are inverse to each other and represent translations in opposing directions. We will describe the disturbances associated with them as "pseudo-acoustic" waves, and we shall see later that these waves obey a leapfrog-like recurrence relationship).

If, as an example, we take $\phi = \tan^{-1} \frac{1}{2}$, so that $C = S^2$, the persistent configuration becomes

$$p = \begin{vmatrix} S^{3/2} - S^{1/2} \\ S^{-3/2} - S^{-1/2} \\ S^{-3/2} + S^{-1/2} - S^{1/2} - S^{-3/2} \\ 0 \end{vmatrix} \quad (5.16)$$

and this is sketched in Fig. 3a. All the waves that are radiated externally from this configuration will be self cancelling. The profiles of pressure and velocity are shown in Fig. 3b. Note that there is never any net change in any quantity across the persistent configuration (unless we add an entropy wave).

For other values of ϕ , the strengths of waves in the persistent configuration remain unaltered, but they are found in different locations. The waves A, B, C, D are displaced from the origin by amounts $\frac{1}{2} a\Delta t(\cos\phi + \sin\phi)$, $\frac{1}{2} a\Delta t(\cos\phi - \sin\phi)$, $\frac{1}{2} a\Delta t(\sin\phi - \cos\phi)$, $-\frac{1}{2} a\Delta t(\cos\phi + \sin\phi)$, and occupy a region of total breadth $a\Delta t(|\cos\phi| + |\sin\phi|)$. As ϕ approaches $N\pi/2$, however, the waves approach and cancel by pairs.

Note that the persistent configuration could be multiplied by any polynomial in the shift operators, to yield another persistent configuration.

We turn now to computing the evolution of arbitrary initial data. By the Cayley-Hamilton theorem we have

$$M^4 - (D + 1)M^3 + 2DM^2 - (D + 1)M + I = 0 \quad (5.17)$$

where

$$D = \frac{1}{2} (C + C^{-1}) + \frac{1}{2} (S + S^{-1}) + \frac{1}{4} (C + C^{-1})(S + S^{-1}) \quad (5.18)$$

so that

$$\tilde{a}_k = (D + 1)\tilde{a}_{k-1} - 2D\tilde{a}_{k-2} + (D + 1)\tilde{a}_{k-3} - \tilde{a}_{k-4} \quad (5.19)$$

is a valid, but tedious recurrence relationship. The trick is to separate \tilde{a} into its steady and unsteady parts, thus

$$\tilde{a} = \alpha p + \beta \tilde{r}_s + g$$

where g lies in ξ , the complement of the space spanned by p and r_s . The argument is formal, treating S and C as real numbers, but any interpretable statements reached in that way must be true.

Introduce the eigenvector factorization of M

$$M = R(\Lambda_p + \Lambda_q)L \quad (5.20)$$

$$= P + Q \quad (5.21)$$

where $\Lambda_p = \text{diag}(1, 1, 0, 0)$ and $\Lambda_q = \text{diag}(0, 0, \lambda_3, \lambda_4)$ where λ_3, λ_4 do not need to be explicitly computed. We then have that

$$Qp = Qr_s = Pg = 0 \quad (5.22)$$

$$Pp = p, \quad Pr_s = r_s.$$

Inserting (5.21) into (5.17) and using (5.22) gives

$$(Q - I)^2(Q^2 - (D - 1)Q + I)g = 0$$

and since $Q - I$ is a non-singular, the part of the solution lying in ξ obeys

$$(Q^2 - (D - 1)Q + I)g = 0 \quad (5.23)$$

or

$$g_k = (D - 1)g_{k-1} - g_{k-2}. \quad (5.24)$$

Thus, the unsteady part of the operator-split Euler solution obeys a recurrence relationship very similar to that found for the abstract problem (cf. 4.15). In the special case $\phi = \pi/4$, we again find a leapfrog-type behavior for the discrete values

$$g_k - 2g_{k-1} + g_{k-2} = \left(\frac{1}{4}\tau^2 + \tau - \frac{5}{2} + \tau^{-1} + \frac{1}{4}\tau^{-2}\right)g_{k-1}. \quad (5.25)$$

This shows that the unsteady part obeys a numerical approximation to $g_{tt} = a^2 g_{xx}$. Fourier analysis reveals a non-dissipative scheme; some lengthy algebra yields the phase speed in a general direction to be

$$a\left(1 + \frac{\sin^2 2\phi}{96} \theta^2\right) + O(\theta^4)$$

which is only slightly in error. The principal disparity between the exact and operator split solutions is this. In both cases an arbitrary initial discontinuity should project into a steady component (one that moves with the fluid) and an unsteady component. The chief failure of the split operators is that they do not correctly distinguish the two sorts of data (except for the entropy wave).

In the exact solution, that part of the data that projects onto the acoustic eigenvectors is treated as unsteady. In the split solution, it is not easy to identify the unsteady part of arbitrary data, but it generally differs from the exact projection. We give here a partial analysis of the decomposition

$$z_0 = \alpha p + \beta r_s + z_0. \quad (5.26)$$

This is facilitated by the observation that M can be symmetrized

$$M = E^{-1} X E \quad (5.27)$$

where

$$E = \frac{1}{\sqrt{2}} \begin{vmatrix} C^{-1/2} & C^{1/2} & 0 & 0 \\ C^{-1/2} & -C^{-1/2} & 0 & 0 \\ 0 & 0 & 1 & 0 \\ 0 & 0 & 0 & \sqrt{2} \end{vmatrix} \quad E^{-1} = \frac{1}{\sqrt{2}} \begin{vmatrix} C^{1/2} & C^{1/2} & 0 & 0 \\ C^{-1/2} & -C^{-1/2} & 0 & 0 \\ 0 & 0 & 2 & 0 \\ 0 & 0 & 0 & \sqrt{2} \end{vmatrix} \quad (5.28)$$

and

$$X = \begin{vmatrix} \frac{1}{8}(C + C^{-1} + 2)(S + S^{-1} + 2) - 1 & \frac{1}{8}(C - C^{-1})(S + S^{-1} + 2) & \frac{1}{4}(C^{1/2} + C^{-1/2})(S - S^{-1}) & 0 \\ \frac{1}{8}(C - C^{-1})(S + S^{-1} + 2) & \frac{1}{8}(C + C^{-1} - 2)(S + S^{-1} + 2) + 1 & \frac{1}{4}(C^{1/2} - C^{-1/2})(S - S^{-1}) & 0 \\ \frac{1}{4}(C^{1/2} + C^{-1/2})(S - S^{-1}) & \frac{1}{4}(C^{1/2} - C^{-1/2})(S - S^{-1}) & \frac{1}{2}(S + S^{-1}) & 0 \\ 0 & 0 & 0 & 1 \end{vmatrix} \quad (5.29)$$

Since the eigenvectors of X will be orthogonal, a formal solution to the problem of determining α, β in (5.26) is

$$\alpha = \frac{p^T E^T E a_0}{p^T E^T E p} \quad (5.30)$$

$$\beta = \frac{\tilde{r}_s^T E^T E a_0}{\tilde{r}_s^T E^T E \tilde{r}_s} = \tilde{r}_s^T a_0 \quad (5.31)$$

and it is only the evaluation of (5.31) that presents any difficulty. Formal manipulations yield

$$\alpha = \frac{-[C^{-1/2}(S^{1/2}-S^{-1/2}), -C^{1/2}(S^{1/2}-S^{-1/2}), \frac{1}{2}(C^{-1/2}-C^{1/2})(S^{1/2}+S^{-1/2}), 0]a_0}{8[1 - (\frac{C^{1/2}+C^{-1/2}}{2})^2 (\frac{S^{1/2}+S^{-1/2}}{2})^2]} \quad (5.30)$$

The denominator of this expression can be expanded as

$$\frac{1}{8} \sum_{n=0}^{\infty} (\frac{C^{1/2}+C^{-1/2}}{2})^{2n} (\frac{S^{1/2}+S^{-1/2}}{2})^{2n} \quad (5.31)$$

For (5.31) there is a coefficient of $C^p S^q$, say, given by a divergent infinite series. However, if (5.31) is multiplied by the numerator of (5.30), all coefficients are given by convergent, hence interpretable, series. For example, if the initial jump consists of an isolated r_x wave, ($a_0 = (1, 0, 0, 0)$) but inclined at $\phi = 45^\circ$ we have $S = C = T$ and

$$\alpha = \frac{T^{-1} - 1}{8} \sum_{n=0}^{\infty} (\frac{T^{1/2} + T^{-1/2}}{2})^{4n} \quad (5.32)$$

The largest coefficients are those of T^{-1} and T^0 . We find

$$C_0 = -C_{-1} = \frac{1}{8} \sum_{n=0}^{\infty} \frac{(4n)!}{(2n)!(2n+1)!} \frac{1}{16^n} \quad (5.33)$$

$$= \frac{1}{8} \sum_{n=0}^{\infty} \frac{(\frac{1}{4})_n (\frac{2}{4})_n (\frac{3}{4})_n (\frac{4}{4})_n}{(\frac{1}{2})_n (\frac{2}{2})_n (\frac{2}{2})_n (\frac{3}{2})_n} \quad (5.34)$$

where $(x)_n = \Gamma(x+n)/\Gamma(x)$ is the Pochhammer symbol. Cancellation of terms

leads to

$$\begin{aligned} c_0 = -c_{-1} &= \frac{1}{8} {}_2F_1\left[\frac{1}{4}, \frac{3}{4}; \frac{3}{2}; 1\right] \\ &= \frac{1}{8} \frac{\Gamma(\frac{3}{2})\Gamma(\frac{1}{2})}{\Gamma(\frac{5}{4})\Gamma(\frac{3}{4})} \\ &= \frac{1}{4} \frac{\Gamma(\frac{1}{2})\Gamma(\frac{1}{2})}{\Gamma(\frac{1}{4})\Gamma(\frac{3}{4})} . \end{aligned}$$

This may be evaluated from the Reflection Formula

$$\Gamma(z)\Gamma(1-z) = \pi/\sin(\pi z)$$

as

$$c_0 = -c_{-1} = \frac{1}{4} \sin(\pi/4). \quad (5.35)$$

The numerical value of these coefficients is 0.177 which could be regarded as the amplitude of the persistent wave configuration generated by the particular initial data. The same amplitude would result from an initial jump proportional to \tilde{r}_x^- and inclined at $\phi = 45^\circ$.

If the initial jump is proportional to \tilde{r}_{vx} and inclined at 45° , then (5.30) yields

$$\alpha = \frac{T-T^{-1}}{16} \sum_{n=0}^{\infty} \left(\frac{T^{1/2} + T^{-1/2}}{2} \right)^{4n}. \quad (5.36)$$

In this expression the coefficient of T^0 vanishes, but the amplitude may be represented by

$$\begin{aligned}
 c_1 = -c_{-1} &= \frac{1}{8} \sum_{n=0}^{\infty} \frac{(4n+1)!}{(2n)!(2n+2)!} \cdot \frac{1}{16^n} \\
 &= \frac{1}{16} \sum_{n=0}^{\infty} \frac{\left(\frac{2}{4}\right)_n \left(\frac{3}{4}\right)_n \left(\frac{4}{4}\right)_n \left(\frac{5}{4}\right)_n}{\left(\frac{1}{2}\right)_n \left(\frac{2}{2}\right)_n \left(\frac{3}{2}\right)_n \left(\frac{4}{2}\right)_n} \quad (5.37) \\
 &= \frac{1}{16} {}_3F_2\left[\frac{3}{4}, \frac{5}{4}, 1; \frac{3}{2}, 2; 1\right].
 \end{aligned}$$

The generalized hypergeometric function appearing here can be summed by Watson's Theorem [5, p. 54], giving

$$\begin{aligned}
 c_1 = -c_{-1} &= \frac{1}{16} \left[\frac{\Gamma(\frac{1}{2})\Gamma(\frac{3}{2})}{\Gamma(\frac{7}{8})\Gamma(\frac{9}{8})} \right]^2 \\
 &= \left[\frac{\Gamma(\frac{1}{2})^2}{\Gamma(\frac{1}{8})\Gamma(\frac{7}{8})} \right]^2
 \end{aligned}$$

which can be evaluated using the Reflection Formula as

$$c_1 = -c_{-1} = \sin^2 \pi/8 = 0.147.$$

Results for arbitrary initial jumps can be found by superposing the special cases, but systematic conclusions would be hard to reach. The important point is that an appreciable fraction of the initial amplitude may be projected onto the persistent wave. This conclusion is reinforced by the numerical experiments in the following section.

6. NUMERICAL EXAMPLES

Fig. 4 shows the distribution of pressure and vertical velocity though the wave system that results from 10 or 30 split time-steps being applied to data representing a shock inclined at $\phi = \pi/4$, i.e., $\underline{a}_0 = (\frac{1}{2}(1 + 1/\sqrt{2}), \frac{1}{2}(1 - 1/\sqrt{2}), 1/\sqrt{2}, 0)^T$. Note that a persistent wave establishes itself very quickly at the center of the domain, where the initial discontinuity was placed. A typical "leapfrog" wave moves to the right in a manner that imitates rather loosely the exact solution (also shown). Some very weak disturbances move to the left.

In Fig. 5 the initial data is a shear wave; $\underline{a}_0 = (0, 1/\sqrt{2}, -1/\sqrt{2}, 0)^T$. Here we see two "pseudo acoustic" waves moving outward, leaving a pronounced persistent pressure defect. The region between is filled with low amplitude noise, especially in the velocity.

Fig. 6 demonstrates that the case $\phi = \pi/4$ is not untypical. Here we take $\phi = \tan^{-1}(\frac{1}{2})$, computing first the data corresponding to a shock ($\underline{a}_0 = (\frac{1}{2}(1 + 2r), \frac{1}{2}(1 - 2r), r, 0)^T$) where $r^2 = 1/5$ and then due to a shear ($\underline{a}_0 = (0, 2r, -r, 0)^T$).

7. RELEVANCE OF STUDY TO PRACTICAL COMPUTATIONS

We have seen that for discontinuous data, the solution of the split problem converges to the solution of the exact problem only in some weak sense, there being $O(1)$ errors even as $\Delta t \rightarrow 0$. That many practical calculations do successfully employ operator splitting is due to just one fact. Two successive wavefronts in the split solution are separated by at most $a\Delta t \min[|\sin\phi|, |\cos\phi|] \leq a\Delta t$. For explicit marching schemes this is

in turn less than the spatial mesh sizes $\Delta x, \Delta y$. In the frequency domain, the difference between the split solution and the true solution lies mostly above the folding frequency and so cannot be resolved by the majority of numerical schemes.

This reasoning does not of course apply to implicit schemes, so any implicit method would have to contain "sufficient" dissipation. Nor does it apply to the explicit "large time-step" schemes developed by Harten [6] and LeVeque [7]. In fact these latter schemes would be particularly inappropriate as they are "high resolution" schemes that aim at preserving high frequencies.

Another scheme that performs very badly in split-operator applications is the Random Choice Method [3]. Again this is because the one-dimensional operator is just too good. The states generated in solving the one-dimensional Riemann problems are not lost in any averaging process, but have a chance to appear in the solution. Although only some of them will appear, there is a striking similarity between the results of the last section and the two-dimensional random choice results in [3]. It is to be expected that other attempts to create "very high resolution" schemes, such as Harten's ACM [8] or Roe's Ultrabee [9] may experience similar difficulties.

More constructively, it is worth noting that any scheme based on decomposition of the data into different waves could use a very-high-resolution operator-split method on those eigenvectors common to both operators, with a slightly less ambitious method employed on the remaining data. In the context of gas dynamics, we might use moderate resolution on the acoustic waves. Shockwaves would nevertheless appear sharp, because they are nonlinear, "self-steepening" phenomena, and expansions would be treated well where they became smooth. The difficult (because linear) entropy waves could be sharpened with-

out creating any splitting problems. Even more valuable, perhaps, would be the application to chemically reactive or multi-phase flows. These always introduce new equations (for the species concentrations) that add more linear wavefields having the same eigenvector in all directions [10]. The ability to use very high resolution schemes on these fields will help to reduce numerical dissipation.

The disturbance that seems most difficult to treat is the shear wave. Because it is linear it is prone to numerical diffusion, but a very high resolution splitting scheme would introduce into the solution the sort of noise displayed in Figs. 5(a-d) and 6(c,d). It may be necessary to control very carefully the degree of resolution applied to these waves, if they are not aligned with any coordinate direction.

REFERENCES

- [1] G. Strang, "On the construction and comparison of difference schemes," SIAM J. Numer. Anal., Vol. 5, pp. 506-517, 1968.
- [2] M. Crandall and A. Majda, "The method of fractional steps for conservation laws," Numer. Math., Vol. 34, pp. 285-314, 1980.
- [3] P. Colella, "Glimm's method for gas dynamics," SIAM J. Sci. Statist. Comput., Vol. 3, pp. 77-110, 1982.
- [4] R. C. Y. Chin and G. W. Hedstrom, "A dispersion analysis for difference schemes: tables of generalized Airy functions," Math. Comp., Vol. 32, pp. 1163-1170, 1978.
- [5] L. J. Slater, "Generalized hypergeometric functions," Cambridge, 1966.
- [6] A. Harten, "On a large time-step high-resolution scheme," ICASE Report No. 82-34, 1982.
- [7] R. LeVeque, "A large time-step generalization of Godunov's method for systems of conservation laws," SIAM J. Numer. Anal., Vol. 22, pp. 1051-1073, 1985.
- [8] A. Harten, "The artificial compression method for computation of shocks and contact discontinuities: III Self-adjusting hybrid schemes," Math. Comp., Vol. 32, pp. 363-389, 1978.

- [9] P. L. Roe and M. J. Baines, "Asymptotic behavior of some nonlinear schemes for linear advection," in Notes on Numerical Fluid Mechanics, M. Pandolfi and R. Piva (ed.), pp. 283-290, Vieweg, 1984.

- [10] H. C. Yee and J. L. Shinn, "Semi-implicit and fully implicit shock-capturing methods for hyperbolic conservation laws with stiff source terms," AIAA Paper 87-1116, July 1987.

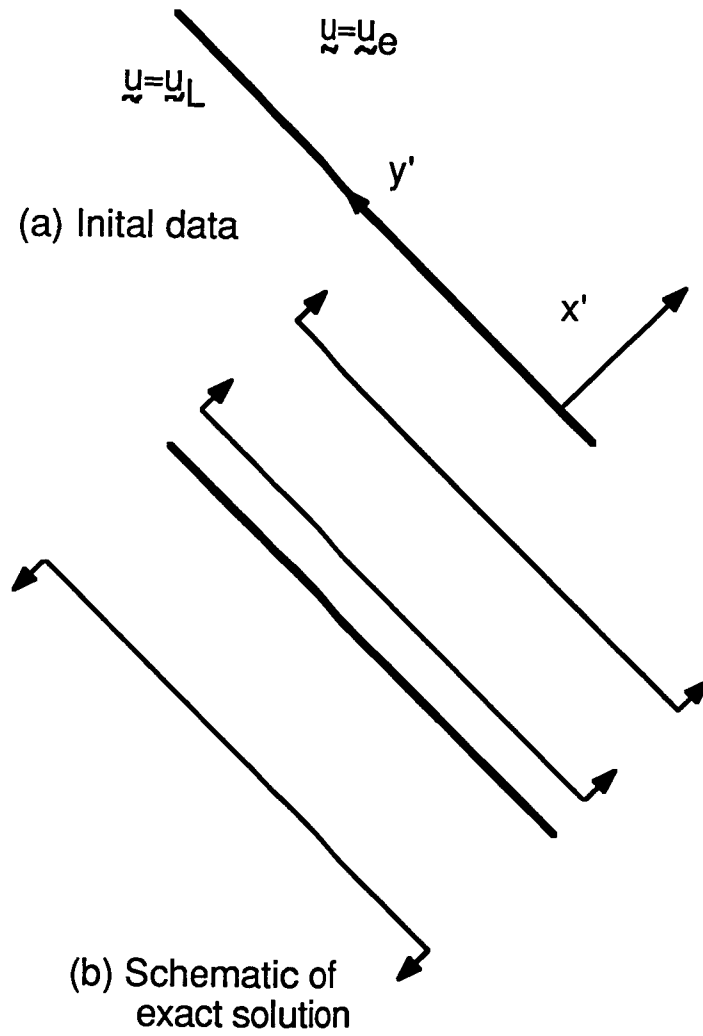
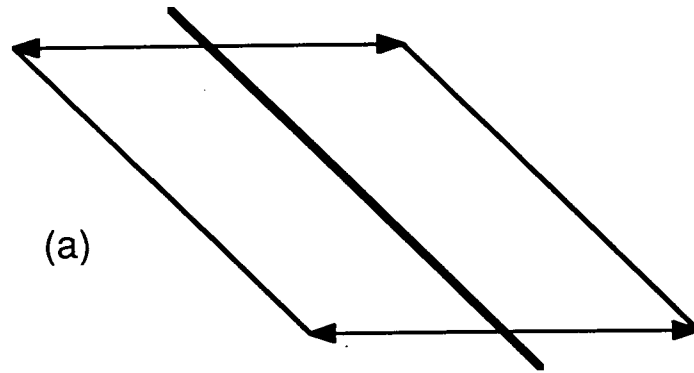
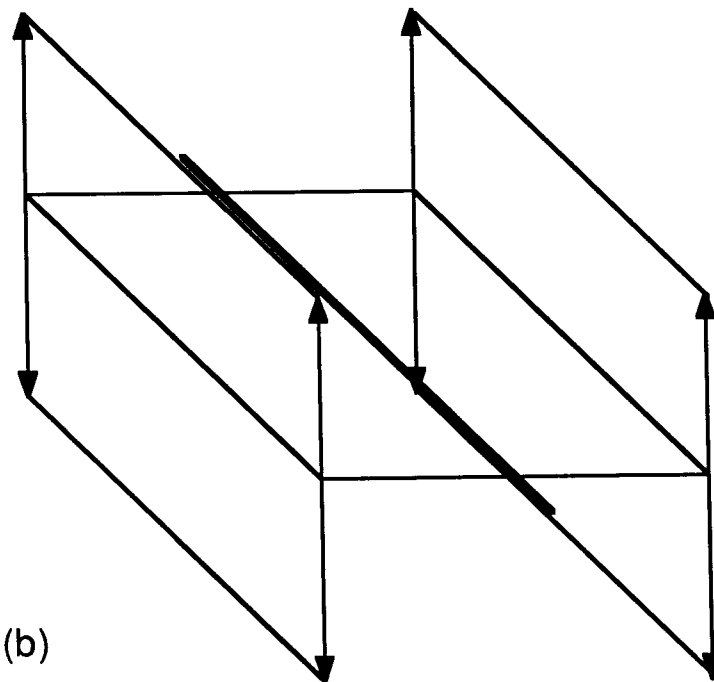


Fig. 1. Breakup of an oblique discontinuity.



(a)



(b)

Fig. 2. Bifurcating wave patterns in the operator-split solution.

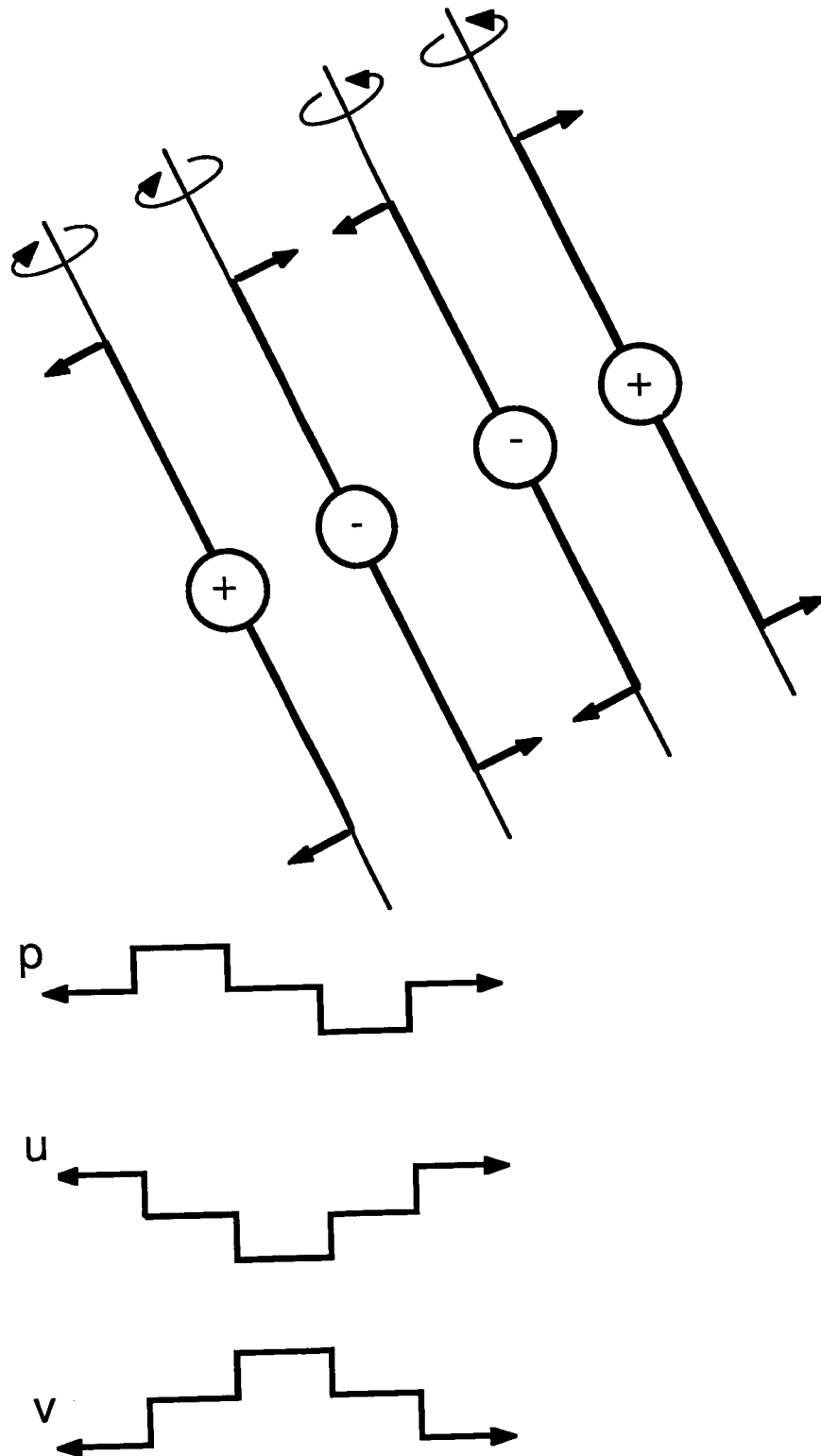
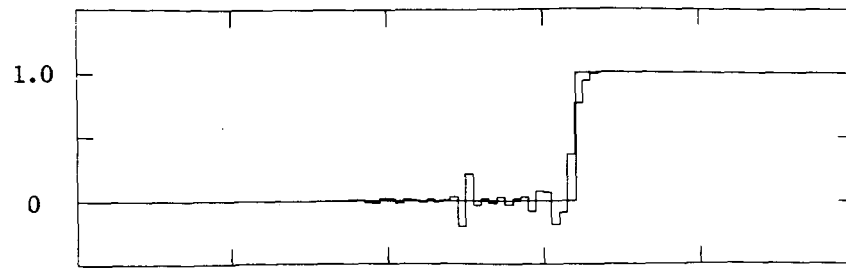
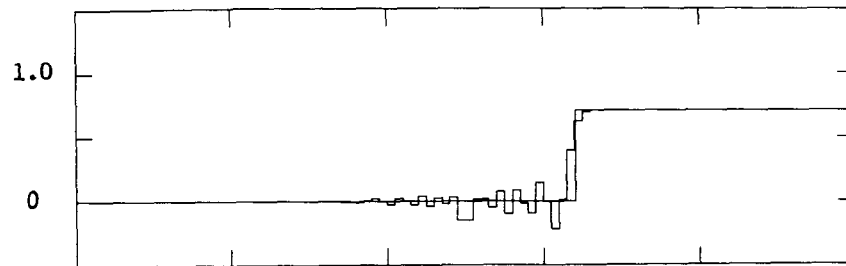


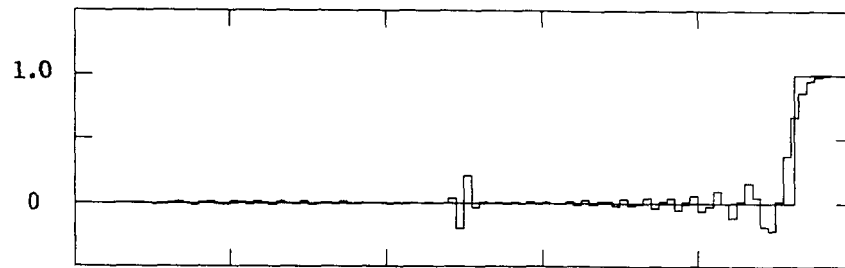
Fig. 3. The persistent wave configuration.



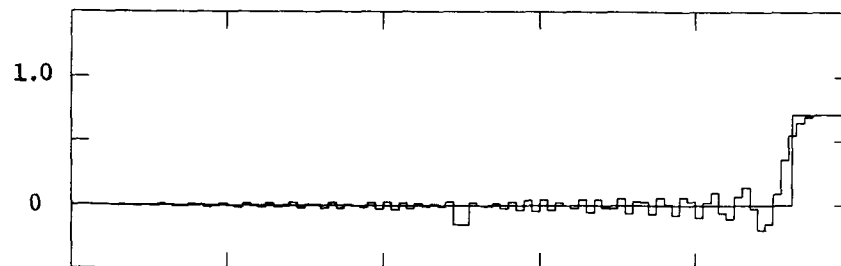
(a) Pressure after 10 steps



(b) Velocity after 10 steps

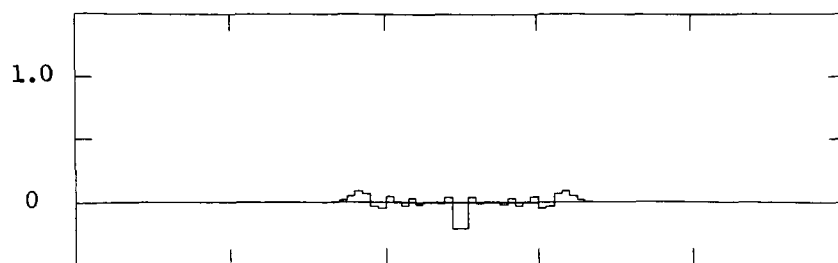


(c) Pressure after 30 steps

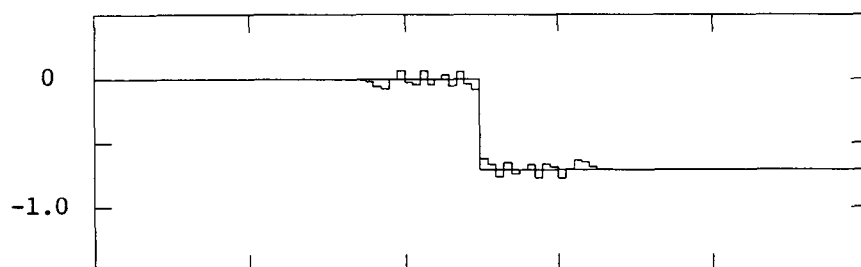


(d) Velocity after 30 steps

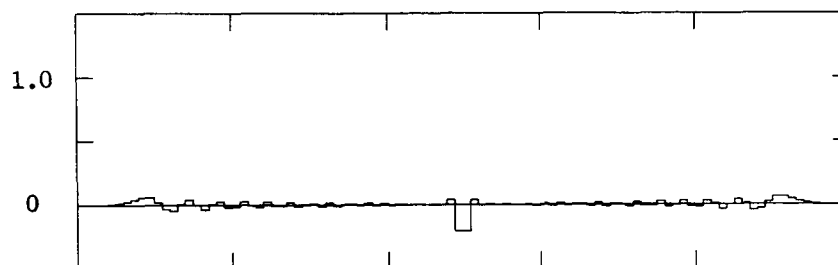
Fig. 4. Results from a shock at $\phi = \pi/4$.



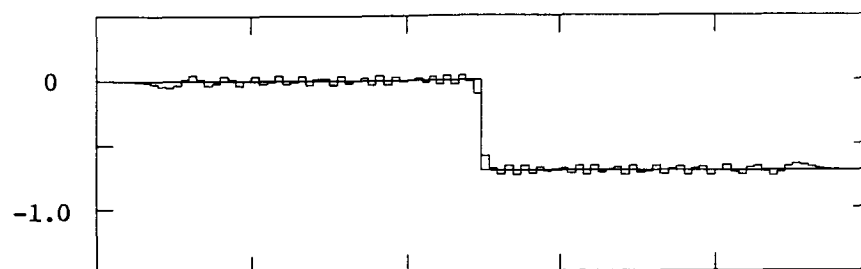
(a) Pressure after 10 steps



(b) Velocity after 10 steps

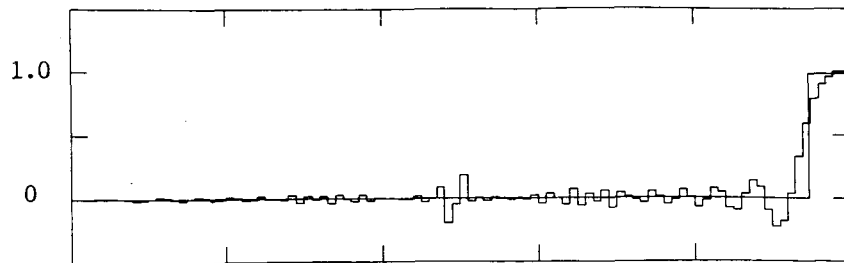


(c) Pressure after 30 steps

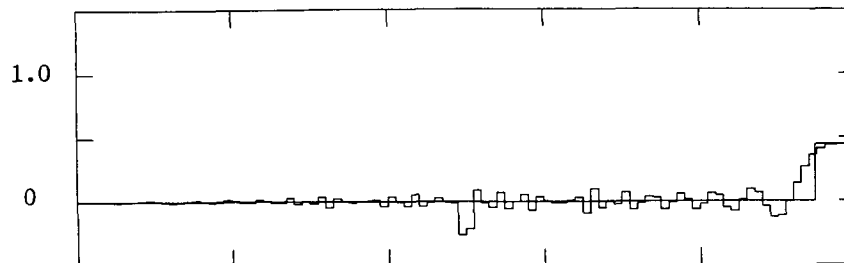


(d) Velocity after 30 steps

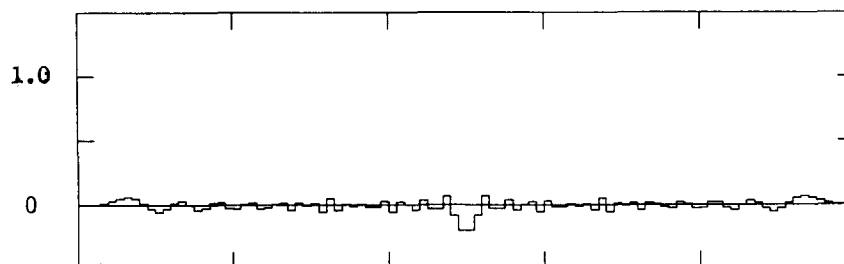
Fig. 5. Results for a shear wave at $\phi = \pi/4$.



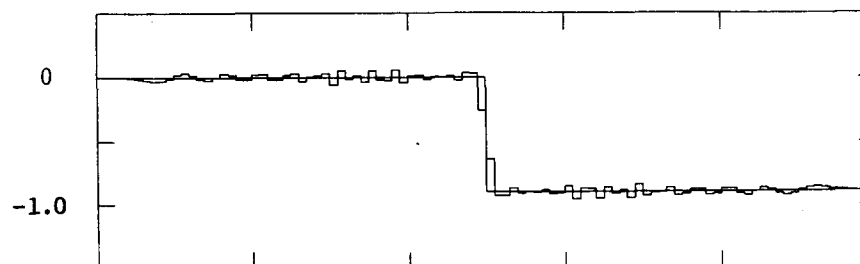
(a) Pressure due to a shock after 20 steps



(b) Velocity due to a shock after 20 steps



(c) Pressure due to a shear after 20 steps



(d) Velocity due to a shear after 20 steps

Fig. 6. Results from waves at $\phi = \tan^{-1} \frac{1}{2}$.

Report Documentation Page

1. Report No. NASA CR-178375 ICASE Report No. 87-64		2. Government Accession No.		3. Recipient's Catalog No.	
4. Title and Subtitle DISCONTINUOUS SOLUTIONS TO HYPERBOLIC SYSTEMS UNDER OPERATOR SPLITTING				5. Report Date September 1987	
				6. Performing Organization Code	
7. Author(s) P. L. Roe				8. Performing Organization Report No. 87-64	
				10. Work Unit No. 505-90-21-01	
9. Performing Organization Name and Address Institute for Computer Applications in Science and Engineering Mail Stop 132C, NASA Langley Research Center Hampton, VA 23665-5225				11. Contract or Grant No. NAS1-18107	
				13. Type of Report and Period Covered Contractor Report	
12. Sponsoring Agency Name and Address National Aeronautics and Space Administration Langley Research Center Hampton, VA 23665-5225				14. Sponsoring Agency Code	
15. Supplementary Notes Langley Technical Monitor: Submitted to SIAM J. Numer. Richard W. Barnwell Anal. Final Report					
16. Abstract Two-dimensional systems of linear hyperbolic equations are studied with regard to their behavior under a solution strategy that in alternate time-steps solves exactly the component one-dimensional operators. The initial data is a step function across an oblique discontinuity. The manner in which this discontinuity breaks up under repeated applications of the split operator is analyzed, and it is shown that the split solution will fail to match the true solution in any case where the two operators do not share all their eigenvectors. The special case of the fluid flow equations is analyzed in more detail, and it is shown that arbitrary initial data gives rise to "pseudo acoustic waves" and a non-physical stationary wave. The implications of these findings for the design of high-resolution computing schemes are discussed.					
17. Key Words (Suggested by Author(s)) discontinuous solutions, operator splitting			18. Distribution Statement 34 - Fluid Mechanics and Heat Transfer 64 - Numerical Analysis Unclassified - unlimited		
19. Security Classif. (of this report) Unclassified	20. Security Classif. (of this page) Unclassified		21. No. of pages 34	22. Price A03	